

Bounding multifractality by observables

Tuomas I. Vanhala, Niklas Järvelin and Teemu Ojanen

*Computational Physics Laboratory, Physics Unit, Faculty of Engineering and Natural Sciences,
Tampere University, P.O. Box 692, FI-33014 Tampere, Finland and
Helsinki Institute of Physics P.O. Box 64, FI-00014, Finland*

Fractal dimensions have been used as a quantitative measure for structure of eigenstates of quantum many-body systems, useful for comparison to random matrix theory predictions or to distinguish many-body localized systems from chaotic ones. For chaotic systems at midspectrum the states are expected to be “ergodic”, infinite temperature states with all fractal dimensions approaching 1 in the thermodynamic limit. However, when moving away from midspectrum, the states develop structure, as they are expected to follow the eigenstate thermalization hypothesis, with few-body observables predicted by a finite-temperature ensemble. We discuss how this structure of the observables can be used to bound the fractal dimensions from above, thus explaining their typical arc-shape over the energy spectrum. We then consider how such upper bounds act as a proxy for the fractal dimension over the many-body localization transition, thus formally connecting the single-particle and Fock space pictures discussed in the literature.

I. INTRODUCTION

Thermalization, chaos, and ergodicity in isolated many-body quantum systems have been frequent topics in recent research [1, 2]. Each of these concepts is an important part of the statistical mechanics of classical systems, and each of them has inspired ways to characterize the eigenstates of many-body quantum systems. The eigenstate thermalization hypothesis (ETH) explains dynamical thermalization by transferring the thermal properties to the eigenstates of the system [1–3], thus giving a characterization of few-body observables. In a chaotic system, away from spectral edges, such observables are expected to approach their thermal expectation values that only depend on the energy of the eigenstate. The observables reveal a structure in the state vector that only vanishes at midspectrum, where the temperature approaches infinity [4] and observables carry no information about the underlying Hamiltonian. This can be contrasted to many-body localized states, where multiple “emergent” integrals of motion are needed to describe the eigenstates [5], and structure is present even at midspectrum. Indeed, it is possible to characterize the many-body localization transition by defining a suitable measure for this structure using e.g. one-particle occupation numbers [6–12].

Another way to quantify structure of eigenstates is to consider the full state vector in a fixed basis. This is conceptually related to studies of quantum ergodicity, where highly excited eigenstates of classically chaotic systems are found to have their weight evenly distributed throughout the phase space [13–15]. In many-body systems, the space-filling properties of midspectrum eigenstates have been compared to eigenstates of random matrix ensembles with symmetry classes appropriate for the underlying Hamiltonian [1]. Common quantitative measures include the inverse participation ratio, and, more generally, Renyi- q entropies S_q of the weight distribution of the state, which have been studied for numerous many-body models [1, 8, 16–25]. Denoting the Hilbert

space size as Q , the complexity of state $|\psi\rangle$ can be expanded as

$$S_q(|\psi\rangle) = D_q \log(Q) + O(1/Q), \quad (1)$$

where D_q is the fractal dimension in the thermodynamic limit. Numerical results indicate that midspectrum states of chaotic systems generally have $D_q = 1$ [17, 26, 27], meaning that the state fills at least a finite fraction of the available Hilbert space in the thermodynamic limit, in agreement with the expectation that these are infinite temperature states with no visible structure in few-body observables. However, as soon as we move away from the infinite temperature point, structure appears and $0 < D_q < 1$ even in a chaotic system. The coefficient D_q attains an arc shape as a function of the energy, decreasing towards the edges of the spectrum [1, 20, 26, 28, 29]. Viewed like this, the state thus becomes “fractal”, with an effective “volume” scaling non-trivially slower than the volume of the space. Similarly, the many-body localized states have $D_q < 1$ even at midspectrum, and numerical scaling analysis indicates that the localization transition may be associated with a jump in the value of D_q in the thermodynamic limit [17]. In either of these cases it is not surprising to find $D_q < 1$, as few-body observables already indicate that the state develops structure, but the exact relation between these two points of view has not fully been explored. Is it possible to predict D_q if few-body observables are assumed to be known?

In this work we discuss how few-body observables can be used to bound the complexity S_q , and thus the fractal dimension D_q , of eigenstates of many-body systems. We define an entropy-like quantity closely related to the occupation number entropy discussed in [6], and show that it bounds the complexity from above, thus supplementing the lower bound relation discussed in our earlier work [30]. We then discuss how tighter bounds can be derived using n :th order density correlations. In chaotic systems, the upper bounds considered here provide a connection between the observables, assumed to follow the ETH, and

the arc shape of the complexity as a function of energy, which we demonstrate numerically. We then study the behaviour of the upper bounds over the localization transition, providing a connection between the single-particle and Hilbert-space descriptions, and discuss how this appears in quench dynamics.

II. UPPER BOUNDS FOR RENYI-COMPLEXITIES

A. Formal setup and derivation of results

In this section we will discuss a class of observable-based measures that can be used to quantify the complexity of a quantum state. If we fix a basis, the state can be expanded as

$$|\psi\rangle = \sum_n a_n |n\rangle, \quad (2)$$

and the corresponding Renyi- q complexities can be defined as the entropies of the weight distribution in this basis,

$$S_q(\vec{p}) = \log \left(\sum_n p_n^q \right) / (1 - q), \quad (3)$$

with the Shannon limit defined as

$$S_1(\vec{p}) = - \sum_n p_n \log(p_n), \quad (4)$$

where $p_n = |a_n|^2$. Suppose now that we have information on this state in the form of expectation values of observables \hat{d}_i diagonal in this basis,

$$\langle \psi | \hat{d}_i | \psi \rangle = \sum_n p_n \langle n | \hat{d}_i | n \rangle = d_i, \quad (5)$$

where the d_i are known values. This knowledge limits the possible complexity, and finding the upper limit corresponds to maximizing the entropy S_q under the constraints given by Eqn. 5 and the additional requirement that the weights form a probability distribution,

$$\begin{aligned} S_q^{max} &= \max_{\vec{p}} S_q(\vec{p}), \\ &\text{subject to} \\ &\sum_n p_n \langle n | \hat{d}_i | n \rangle = d_i, \quad i = 1 \dots N. \\ &p_n \geq 0, \quad n = 1 \dots Q \\ &\sum_n p_n = 1 \end{aligned} \quad (6)$$

This is generally a convex optimization problem that can be solved numerically [31], and we will present results for small enough systems below. However, in the case

of the Shannon entropy S_1 it is also possible to find analytical results based on the similarity of this problem to standard thermodynamics. In App. A we consider a fermionic system, and assume that the average occupation of each of the orbitals is known, i.e. that \hat{d}_i are the occupation number operators $\hat{d}_i = \hat{n}_i$. We denote the resulting maximum complexity as $S_1^{max,n} \geq S_1$. As shown in the appendix, $S_1^{max,n}$ then has an upper bound that is formally the same as the grand canonical entropy of free fermions,

$$\begin{aligned} S_1^{max,gc} &= - \sum_i (n_i \log(n_i) + (1 - n_i) \log(1 - n_i)) \\ &\geq S_1^{max,n} \geq S_1, \end{aligned} \quad (7)$$

where n_i are the average occupations of the orbitals. The bound is larger than the exact $S_1^{max,n}$ because it neglects particle conservation constraints that are typically preserved by the Hamiltonian, and which we tacitly assume to hold in Eq. 6. Noting the general inequality $S_{q_1} \leq S_{q_2}$ for $q_2 < q_1$, we also see that $S_1^{max,n}$ bounds all Renyi-complexities from above. While we only consider fermions here, we also note that the discussed ideas are more general and analogous bounds can be derived e.g. for bosonic or spin-systems.

$S_1^{max,gc}$ yields immediately an upper bound also for the fractal dimension D_1 as $D_1^{max,gc} = S_1^{max,gc} / \log(Q)$, where Q is the number of basis states. Due to the neglected particle conservation, this bound is generally not very tight for numerically attainable system sizes, and can even yield values larger than 1. However, as shown in App. A, the thermodynamic limit of the bound, which we call $D_1^{max,lim}$, can be expressed as

$$\begin{aligned} D_1^{max,lim} &= \lim_{N_o \rightarrow \infty} D_1^{max,gc} \\ &= \frac{\lim_{N_o \rightarrow \infty} \frac{1}{N_o} S_1^{max,gc}}{-\nu \log(\nu) - (1 - \nu) \log(1 - \nu)}, \end{aligned} \quad (8)$$

where N_o is the number of orbitals and ν is the overall filling fraction of the system. Thus it is the intensive quantity $S_1^{max,gc} / N_o$ that determines the upper bound for large systems, always yielding $\lim_{N_o \rightarrow \infty} D_1^{max,gc} \leq 1$. Below we use $D_1^{max,lim}$ also for finite systems with the understanding that $\lim_{N_o \rightarrow \infty} S_1^{max,gc} / N_o$ is approximated from a system with finite N_o . It is also important to note that $S_1^{max,gc} - S_1^{max}$ is not expected to converge to zero even for arbitrarily large systems due to the neglected particle conservation, but instead may diverge. However, $D_1^{max,gc}$ and D_1^{max} are expected to converge to the same value, as the error grows slower than N_o . In practice we find that $S_1^{max,gc} / N_o$ converges faster than $S_1^{max,gc} / \log(Q)$, and thus Eq. 8 is preferred for estimating the thermodynamic limit, as numerically demonstrated below.

One can also consider complexity bounds under constraints on higher order correlation functions. For example, we can set $\hat{d}_i = \hat{n}_{\mu_i} \hat{n}_{\nu_i}$, asking for the highest

possible complexity when the density-density correlators are known, or $\hat{d}_i = \hat{n}_{\mu_i} \hat{n}_{\nu_i} \hat{n}_{\gamma_i}$ if the third order correlators are known, and so on. We denote these higher order bounds as $S_q^{max,nn}$, $S_q^{max,nnn}$, etc. As discussed in App. A, computing these bounds from the correlation functions requires solving classical lattice gas problems which do not have an analytical solution, and thus we cannot hope for a similar simple formula as in the case of one-particle constraints, but the bounds can still be computed numerically.

B. Discussion and comparison to earlier results

The expression for $S_1^{max,gc}$ can be compared with the ‘‘occupation number entropy’’

$$S_{occ} = - \sum_i n_i \log(n_i), \quad (9)$$

used in Ref. [6] to quantify the numerically observed transition in the single-particle occupation spectrum of the natural orbitals when crossing the many-body localization transition. Qualitatively, S_{occ} and $S_1^{max,gc}$ very similarly measure the uniformity of the occupation distribution, but $S_1^{max,gc}$ is particle-hole symmetric. The relation $S_1^{max,gc} \geq S_1$ gives additional support to the idea that such single-particle quantities can be used to characterize the many-body localization transition, as it formally relates the single-particle and Fock-space pictures.

The natural orbitals, defined as eigenorbitals of the one-particle reduced density matrix [32], have been studied as a basis where the full state vector has a compact representation [32?–37]. As briefly discussed in App. B, both $S_1^{max,gc}$ and S_{occ} have the property that, among all possible choices of single-particle orbital sets, they attain their minimum value in the natural orbital basis. This is one sense in which the natural orbital basis is optimal: It does not necessarily give the lowest complexity S_1 , but it has the lowest upper bound to the complexity if only the one-particle reduced density matrix is known.

Another relevant single-particle quantity is the local polarization [38] of spin systems, or its fermionic analogue, the ‘‘local purity’’ [8],

$$S_{lp} = \frac{1}{N_o} \sum_i (2n_i - 1)^2, \quad (10)$$

which can be expressed in terms of the expectation value of the Hamming distance x_{ij} between the basis states i and j [8],

$$S_{lp} = 1 - \frac{2}{N_o} \sum_{ij} x_{ij} p_i p_j. \quad (11)$$

The local purity has been related to the second Renyi-complexity S_2 , but the exact relationship requires more information on the state than the upper bound relation

discussed above for the Shannon entropy. In the many-body localized state the eigenstates typically concentrate around one Fock configuration, and the weights decay exponentially with increasing Hamming distance between the occupation number sets [39], which leads to a linear relationship between S_{lp} and the inverse participation ratio $\exp(S_2)$ [38]. Numerically a relationship between S_{lp} and related quantities and S_2 is observed also e.g. for eigenstates of many-body Hamiltonians and random matrix ensembles [30]. It is thus an interesting question whether the solution to Eq. 6 with $q = 2$ can be expressed in terms of the local purity similarly to how the $S_1^{max,gc}$ provides the limit for the $q = 1$ case. However, we are unaware of any useful analytical solutions for the optimization problem Eqn. 6 for $q > 1$.

III. NUMERICAL RESULTS

The problem 6 is a convex optimization problem whose global optimum can be found using numerical methods [31]. Here we have employed the QuSpin library for building the Hamiltonian matrices and for finding the eigenstates [40, 41], and the CVXOPT-library [42] for solving the optimization problem. We perform the optimization either with single-particle conditions, where the density expectation values are assumed to be known, and with two-particle conditions where density-density correlation functions between all orbitals are given. We also present some results with three-particle conditions, where all density-density-density correlations are known, but naturally the optimization problem becomes more difficult to solve with increasingly complex conditions. We note that, because of the particle conservation, the n -particle conditions imply the $n - 1$ particle conditions, and thus always result in a stricter bound. In practice we first solve a selected eigenstate of the system, which allows us to compute the weights p_i , the exact S_q , the occupations $\langle n_i \rangle$, and the higher correlation functions, and then proceed to the optimization. We discuss results for the Shannon entropy S_1 and the Renyi-2 entropy S_2 .

We demonstrate the upper bounds for the $t - V$ -model defined as

$$H = \sum_{\langle i,j \rangle} \left(-t \left(\hat{c}_i^\dagger \hat{c}_j + \text{h.c.} \right) + V \left(\hat{n}_i - \frac{1}{2} \right) \left(\hat{n}_j - \frac{1}{2} \right) + \epsilon_i \left(n_i - \frac{1}{2} \right) \right), \quad (12)$$

where we set $t = \frac{1}{2}$ and $V = 1$. The random on-site potential ϵ_i is taken to be uniformly distributed in the interval $[-W, W]$. For small enough $W \lesssim 3$ the model is in a chaotic, thermalizing phase. When W is increased, the model transitions into the many-body localized region, although the exact nature and location of the localization transition is still under debate [43]. Here we will first discuss the arc-shaped form of the fractal dimen-

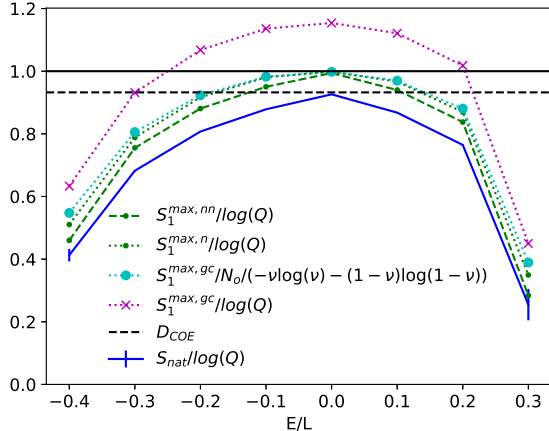


FIG. 1. Fractal dimension D_1 and different upper bound estimates for the t - V model in the natural orbital basis. The model is in the chaotic phase with $t = W = V = 1.0$ and the chain length is $L = 18$. The results are computed as the mean over 1000 random potential realizations at each energy, with the (small) error bars on $D_1 = S_{nat}/\log(Q)$ showing the standard error. The horizontal lines demarcate the trivial bound $D_1 = 1$ and the result for the circular orthogonal ensemble.

sions as a function of the energy in the chaotic phase, and then study the localization transition.

A. Chaotic phase

Fig. 1 shows the fractal dimension D_1 and the associated one- and two-particle bounds for the $t - V$ model in the chaotic phase. The fractal dimension shows the typical arc shape, with an apex at $E/L \approx 0$ in agreement with the fact that the expected energy per length unit of the system approaches zero at infinite temperature in the large system limit. The loosest bound is the grand canonical approximation to the single-particle bound, which, at this system size at midspectrum, is well above the trivial bound $D_1 \leq 1$. However, the thermodynamical limit formula, Eq. 8, closely follows the numerically computed single-particle bound that takes into account particle conservation. This shows that, already at this small system size, Eq. 8 provides a useful upper bound estimate. The two-particle bound is somewhat tighter than the one-particle bound, but the improvement in this case is not drastic. This is understandable, because the system with $V = 1$ is weakly correlated. In the limit of small V we may expect that Hartree-Fock mean-field theory gives a good description of the correlation functions, which implies that the two-particle correlations factorize and thus give no additional information on the state.

It is interesting to discuss how tight the bounds considered here can become. If we consider generic n -particle conditions on the weight distribution, the bound be-

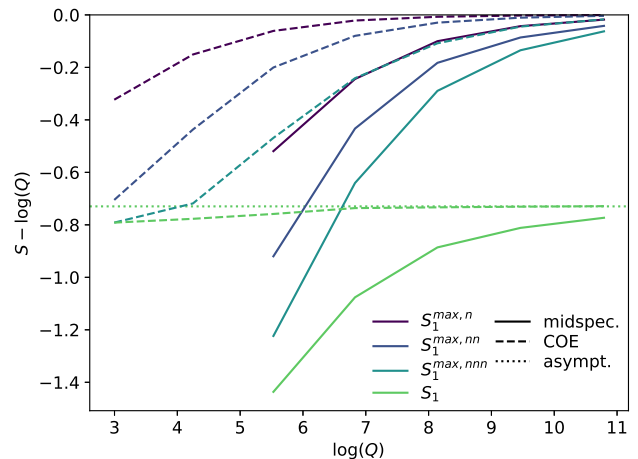


FIG. 2. The complexity S_1 and its 1, 2 and 3-body upper bounds as a function of the system size for the COE and the $t - V$ model at midspectrum. The results are computed in the natural orbitals, and averaged over 1000 disorder realizations. For each disorder realization of the $t - V$ model we compute the mean energy in the canonical ensemble at infinite temperature, and then select an eigenstate close to this energy. According to the ETH, this is expected to yield states that have no few-body structure in the thermodynamic limit. We have subtracted the trivial contribution $\log(Q)$ from all plotted quantities to better show the differences. For the COE, S_1 approaches the asymptotic result $S_1 = \log(Q) - c$, with c a known constant.

comes tighter with increasing n , giving the exact S_q when $n = N_p$. However, the interesting limit is rather the case where n is small and fixed and the system size approaches infinity, i.e. the “few-body” limit. According to the eigenstate thermalization hypothesis, the few-body observables in large systems should be predicted by a thermal (microcanonical or canonical) ensemble [1–3], and thus the upper bounds only depend on the energy or temperature. At “midspectrum”, where the temperature is infinite and observables show no structure, all such few-body bounds should approach the trivial bound $S_q^{max} = \log(Q)$. However, the actual complexity, S_q , does not approach the trivial bound as the state generally contains structure not seen in few-body observables. A common assumption is that the structure can be described by the eigenstates of a random Hamiltonian ensemble that respects symmetries of the problem, such as the gaussian orthogonal ensemble (GOE) when the only relevant symmetry is time-reversal [1, 26]. For the GOE eigenstates (distributed according to the circular orthogonal ensemble (COE)), the large- Q limit is given by $S_1 \approx 1 - c$, where $c \approx (\log(2) + \psi(3/2))$ and ψ is the digamma function [26]. Thus we may expect that a gap, representing “random fluctuations” not captured by few-body observables, remains between S_q and the n -body bounds regardless of n , as long as $n \ll N_p$. The question is if this gap generally remains bounded, as expected at

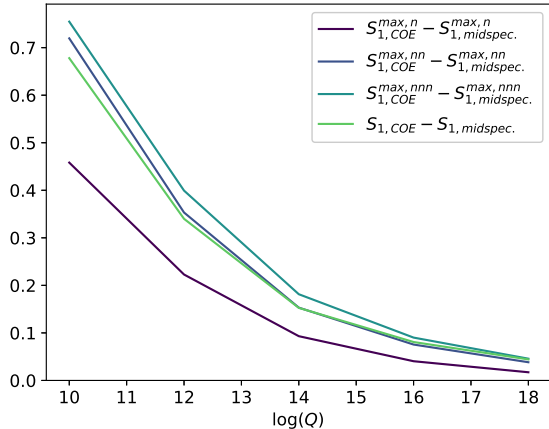


FIG. 3. Difference between the corresponding COE and $t-V$ model quantities of Fig. 2.

midspectrum, or if it grows linearly, leading to a constant gap in the fractal dimension in the thermodynamic limit. We will consider this question below, but we first present numerical results at midspectrum.

To test the above picture at midspectrum, we compare the upper bounds and complexities of the $t-V$ model to those of COE-distributed states in Fig. 2. As has been noted for other models in the literature [26], the finite-size corrections to S_1 , or to the fractal dimensions, generally differ from the random matrix predictions. This is observed also here, as the complexity of the COE states converges much faster to the asymptotic result $S_1 \approx \log(Q) - c$ compared to the $t-V$ model. Interestingly, the same behaviour is seen also in the upper bounds: The n -particle bound for the COE approaches $\log(Q)$ faster than for the $t-V$ model. Thus we can conclude that the slower approach to the thermodynamic limit is due to the few-body correlations present in the $t-V$ eigenstates, and the upper bounds provide an economical measure of such correlations. Such structure is expected, since the $t-V$ Hamiltonian, and indeed most physical Hamiltonians, are composed of few-body terms. This can be compared to earlier results on the XYZ spin chain showing that residual spatial correlations can reduce the midspectrum entanglement entropy in finite systems [29].

We also plot the difference of the upper bounds between the COE states and the $t-V$ model in Fig. 3, thus measuring the excess of n -body structure in the $t-V$ model eigenstates compared to the COE states. Notably, this excess for the two- and three-body bounds roughly corresponds to the difference of the actual complexities between the two systems. This supports the idea that the complexity can be thought of as a sum of two terms: A term arising from a few-body structure, which is smaller for the $t-V$ model compared to the COE states, and a random term which is similar for the two models.

Moving away from the infinite temperature point, we compare the scaling of the upper bounds and the true complexity at fixed specific energies. Here the most interesting question is if the gap between the true complexity and the upper bounds saturates to a finite value, or if it tends to infinity in the large system size limit. The complexity and the upper bounds are plotted in Fig. 4. The gap generally increases with system size, but, plotted against $1/\log(Q)$, it does not appear divergent, especially considering the two-particle bound. Thus it seems plausible that the few-body bounds can correctly predict the fractal dimension of the state in the infinite system size limit, with a constant gap remaining between the bound and the complexity. Intuitively, the few-particle structure limits the Hilbert space volume available to the state to a fraction of the total volume Q , and this fraction vanishes in the thermodynamic limit, except for the infinite temperature states. The states, however, fill some finite fraction of that limited volume, which is reflected in the size of the gap. This remaining gap represents a “randomness” of the state that cannot be captured by few-body observables. This picture summarizes our “hypothesis of the arc” that relates the complexity in chaotic systems to few-particle observables predicted by the ETH.

B. Localization transition

The existence, nature and location of many-body localization transitions in the thermodynamic limit are still not fully understood [43]. In finite systems accessible by exact diagonalization methods the transition is clearly signalled by the level spectrum, the eigenstate fractal dimensions and single-particle observables [6, 43]. Scaling analyses indicate that the fractal dimension undergoes a non-universal jump at the transition point [17], thus sharply defining the transition. However, due to the system size limitations, the correct scaling ansatz has not been definitively identified, and it is typical that the transition point seems to “creep” to higher disorder strengths with sufficiently large system sizes [43]. Thus the possibility remains that this is not a true phase transition, but a crossover that moves to infinite disorder strengths in the thermodynamic limit. Here we do not attempt to solve this long-standing puzzle, but to discuss how the localized states at attainable system sizes are characterized by the upper bounds.

Fig. 5a shows the fractal dimension D_2 and its upper bounds at midspectrum as the disorder strength is increased from the chaotic region. We discuss here the Renyi-2 case as has been previously considered in the context of MBL [8, 38] and because we find the optimization problem, Eqn. 6, numerically harder to solve for the $q = 1$ case in the localized region. The behaviour in the chaotic region at midspectrum parallels that of the Renyi-1 case with the upper bounds approaching $S = \log(Q)$, and the complexity S_2 retaining a gap below

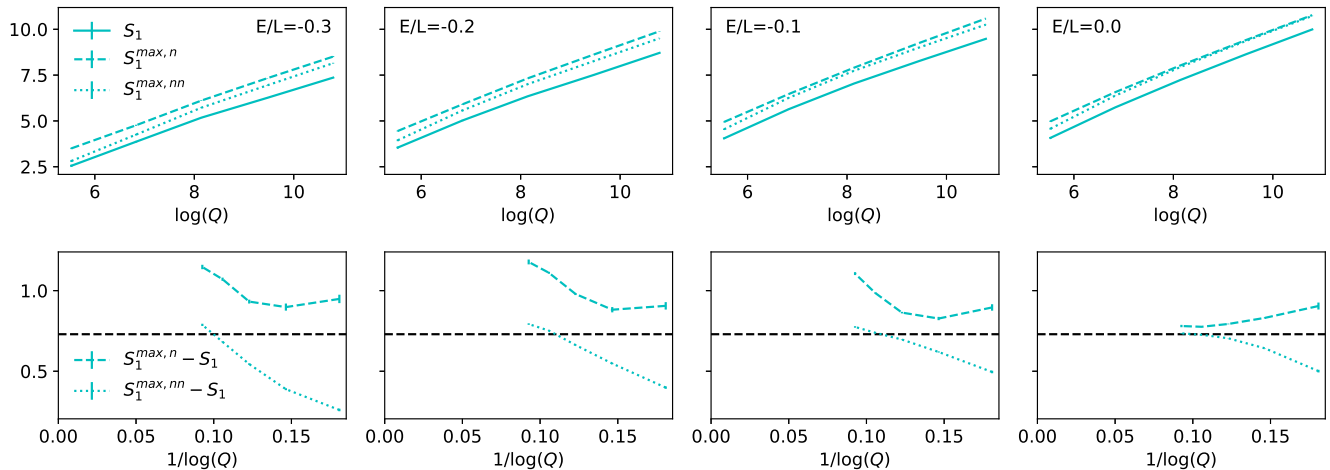


FIG. 4. Upper panels: Complexity S_1 and its one- and two-particle upper bounds as a function of the logarithm of the Hilbert space dimension in natural orbital basis. Lower panels: The gap between the actual complexity and the upper bounds. The dashed black line is the asymptotic COE gap c . The results have been averaged over 100 disorder realizations away from $E = 0$ and 1100 realizations at $E = 0$, except for the largest system size $L = 18$ where we used only 10 realizations in all cases. The standard error is indicated where it is larger than the line width.

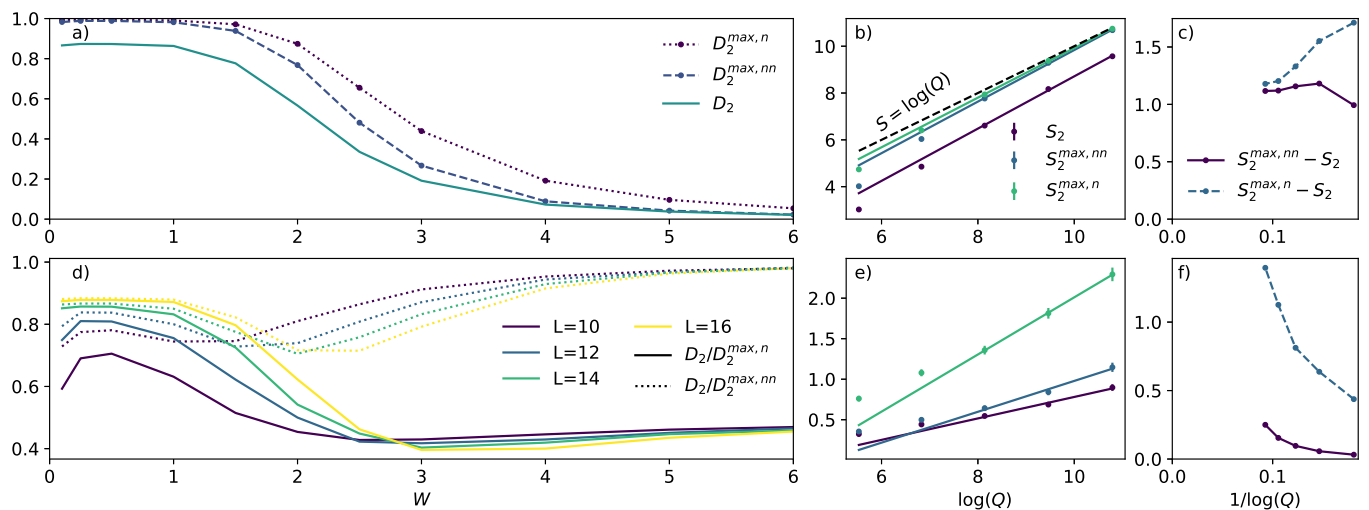


FIG. 5. Complexity upper bounds over the localization transition in the natural orbital basis. a) The midspectrum ($E/L = 0$) fractal dimension D_2 and its upper bounds for a system of size $L = 16$ computed as a mean over 1000 disorder realizations. b) System size dependence of the Renyi-2 complexity S_2 and its upper limits at $W = 1$ (chaotic system). Solid lines are linear fits to the 3 rightmost points. c) The gap between the bounds and the actual complexity S_2 as a function of $1/\log(Q)$ similarly as in Fig. 4. d) The mean ratio of the true fractal dimension to the upper bounds for different system sizes. e-f) As in b-c but for $W = 4$ (localized region).

the bounds that approaches a finite value, as shown in Fig. 5b and 5c. The fractal dimension $D_2 = S_2/\log(Q)$ thus converges to $D_2 \approx 1$ in the chaotic region as expected.

In contrast to the chaotic region, the localized region shows a clear decrease in the estimated fractal dimension and the upper bounds, resembling the occupation number entropy of reference [6]. Another difference to the chaotic case is that the fractal dimension predicted by the upper bounds is now clearly higher than the true

fractal dimension in the large system limit. This is seen e.g. in Fig. 5d where the ratio of D_2 to its upper bounds is plotted. In the chaotic region these ratios increase with increasing system size, while for large enough disorder strength they start to decrease. In other words, the bounds $S_2^{\max,n}$ and $S_2^{\max,nn}$ in the localized region grow faster than the true S_2 , and the gap between S_2 and the bounds increases proportionally to $\log(Q)$, as seen in Fig. 5e and 5f. This can be contrasted to the results in the chaotic phase shown in Fig. 4, where the increase is

slower and the gap appears to approach a finite value in the infinite system size limit.

The natural orbitals can be seen as a single-particle approximation to the emergent integrals of motion characterizing the localized states, especially deep in the localized region [7]. In this region the natural occupation spectrum resembles a fermi-liquid state with one highest-weight Slater configuration and a discontinuity at the “fermi surface” [7]. In contrast, the occupation spectrum in the chaotic region resembles a finite-temperature fermi distribution and the discontinuity is expected to vanish in the thermodynamic limit. Consistently with this picture, the one-particle bound, which is related to the ensemble of free fermions (see App. A), is relatively close to the two-particle bound in the chaotic region, while the two-particle conditions give a significant improvement in the localized region. We can also say that the two-particle correlations, resulting from interaction effects, are much more important in the localized region.

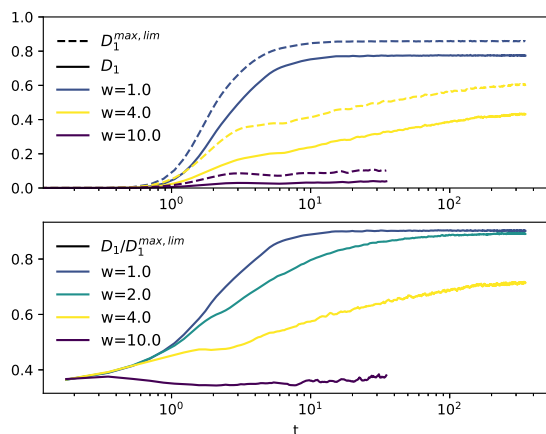


FIG. 6. Upper panel: Time development of the mean fractal dimension and the thermodynamical limit formula, Eq. 8 in the natural orbital basis. The system starts from the Slater state with alternating occupations $|010101\dots\rangle$ and is time developed with the $t - V$ Hamiltonian of length $L = 14$ with varying disorder strength. The results are averaged over 100 disorder realizations. The limit $\lim_{N_o \rightarrow \infty} S_1/N_o$ is estimated directly from the data at this system size. Lower panel: ratio of the complexity and the limit formula.

We finally consider the behaviour of the fractal dimension and the upper bounds for quenches starting from a Slater determinant state. Such quenches have been used in numerical experiments e.g. to investigate the relationship between dynamics of the entanglement entropy and physical observables [44]. Here we want to see if the one-body bound $D_1^{max,lim}$ acts as a proxy quantity to the fractal dimension D_1 as it does for the eigenstates. Indeed, as shown in Fig. 6, these quantities qualitatively follow each other, starting from zero in a Slater configuration and developing into a plateau with slowly increasing complexity. This slow increase may be another symptom

of the “creeping” phenomenon where the system slowly seems to develop towards the chaotic system (large complexity) even for large disorder strengths, where the complexity initially seems to saturate to lower values.

IV. SUMMARY AND OUTLOOK

In this work we have discussed how structure measured in few-body observables limits the complexity and fractal dimensions of eigenstates of many-body systems. By analogy to a thermal free-fermion system, we derived an upper bound for the Shannon-type fractal dimension $D_1 \leq D_1^{max,lim}$ (Eq. 8), which requires the knowledge of the occupation numbers in the chosen orbital basis. In our chaotic model system the formula predicts the arc shape of D_1 as a function of energy quite well. The bound can be improved if information on higher order correlation functions, such as density-density correlations, is available, which leads to a series of bounds with increasing correlator order. For weakly coupled chaotic systems, where few-body correlators are well described by thermal mean-field theory, the higher order correlators factorize and therefore give no additional information, and thus the lowest order bound D_1 is expected to be quite tight. This argument is based on the ETH, i.e. that few-body observables are assumed to follow thermal averages, and one motivation for our study is to connect the thermally predicted observables to the complexity.

We also considered how the upper bounds can be used to locate and characterize the many-body localization transition. In earlier literature the transition has been characterized using both single-particle quantities and fractal dimensions [1, 6–8, 16–25]. Our work formally connects these two pictures, as deviation of e.g. the one-body upper bound from the maximal value immediately implies non-ergodicity of the state (i.e. fractal dimension $D_1 < 1$). Furthermore, the higher order bounds act as a measure of correlation, separating the localized states from mean-field-like, weakly correlated states. We also showed that the one-body bound acts as a more easily studied proxy-quantity to the complexity and fractal dimension in a dynamical setting, which could be useful e.g. in ultracold gas experiments.

To further understand behaviour of the derived bounds in the thermodynamic limit, we analyzed their system size scaling first in the chaotic model. At midspectrum, where few-body observables are given by the infinite-temperature ensemble, all few-body bounds S_1^{max} approach $\log(Q)$ in the thermodynamic limit and the gap $S_1^{max} - S_1 \rightarrow c$, where c is well predicted by a suitable random matrix ensemble respecting the symmetries of the system. However, as noted in the literature, the finite-size scaling of S_q and D_q are system dependent and deviate from the COE predictions [26]. Here we employed the 1-, 2- and 3-body bounds to show that our model system has an excess of few-body correlations compared to the COE, explaining the slower approach to the ther-

modynamic limit. The bounds thus act as a measure of correlations that are useful for characterizing deviations from random matrix predictions.

When moving away from midspectrum to finite temperature states, it still seems that the gap between the actual complexity and the few-body bounds remains bounded in the thermodynamic limit, $S_1^{max,nn} - S_1 \rightarrow C$ for example. This also means that the fractal dimension D_1 in the thermodynamic limit is exactly predicted by the corresponding bound $S_1^{max,nn} / \log(Q)$. While the bound $S_1^{max,nn}$ represents a limitation to the “volume” of the state set by the thermal correlations, the gap C includes the contribution of “random fluctuations” not visible in any few-body observables, and remains similar in magnitude to the gap at midspectrum. An interesting interpretation is thus that eigenstates in a chaotic system are still “random states” even away from midspectrum, but now within the limitations of the few-body observables prescribed by the ETH, although the precise definition of the random ensemble in question remains a subject for future work. The above picture is different in the localized region of our model, where it seems that the gap between the few-body bounds and the complexity grows linearly with $\log(Q)$ and thus the fractal dimension is not exactly given by the respective upper bounds. The intuitive picture is thus that the “volume” of the state grows slower than expected from the bounds.

We note that the conclusions on the scaling behaviour of the bounds are based on exact diagonalization calculations with limited system sizes, and further results from

different model systems would be desirable to confirm the picture. In the chaotic phase, under assumption of the ETH, it may be possible to study the bounds via e.g. Monte-Carlo calculations, as they only require knowledge of selected observables instead of the full state vector. In such calculations the complexity itself remains unknown, but calculating successive n -body bounds might reveal interesting information.

In summary, we have considered a new class of upper bounds to the complexity that are useful for understanding the arc-shape of the fractal dimension as a function of energy in chaotic systems, can be employed as a measure of correlations to analyze deviations from random matrix predictions, and to formally connect the observable-based and fractal-dimension-based pictures of many-body localization. We thus expect these quantities to give new insights in the study of quantum chaos and many-body localization. An interesting idea for future development would be to try to formulate a refined random matrix model where the one-body or few-body bounds could be tuned by parameters to model states away from midspectrum in a chaotic system. As another future direction it would be interesting to consider the complexity and its upper bounds as internal time scales of quench dynamics similarly to the entanglement entropy in [44].

ACKNOWLEDGMENTS

The authors acknowledge the Academy of Finland project 331094 for support. Computing resources were provided by CSC – the Finnish IT Center for Science.

-
- [1] L. D’Alessio, Y. Kafri, A. Polkovnikov, and M. Rigol, From quantum chaos and eigenstate thermalization to statistical mechanics and thermodynamics, *Adv. Phys.* **65**, 239 (2016).
 - [2] J. M. Deutsch, Eigenstate thermalization hypothesis, *Rep. Prog. Phys.* **81**, 082001 (2018).
 - [3] M. Srednicki, Chaos and quantum thermalization, *Phys. Rev. E* **50**, 888 (1994).
 - [4] P. C. Burke, G. Nakerst, and M. Haque, Assigning temperatures to eigenstates, *Phys. Rev. E* **107**, 024102 (2023).
 - [5] J. Z. Imbrie, V. Ros, and A. Scardicchio, Local integrals of motion in many-body localized systems, *Annalen der Physik* **529**, 1600278 (2017), [arXiv:1609.08076 \[cond-mat.dis-nn\]](https://arxiv.org/abs/1609.08076).
 - [6] S. Bera, H. Schomerus, F. Heidrich-Meisner, and J. H. Bardarson, Many-body localization characterized from a one-particle perspective, *Phys. Rev. Lett.* **115**, 046603 (2015).
 - [7] S. Bera, T. Martynek, H. Schomerus, F. Heidrich-Meisner, and J. H. Bardarson, One-particle density matrix characterization of many-body localization, *Annalen der Physik* **529**, 1600356 (2017), [arXiv:1611.01687 \[cond-mat.dis-nn\]](https://arxiv.org/abs/1611.01687).
 - [8] T. Orito and K.-I. Imura, Multifractality and fock-space localization in many-body localized states: One-particle density matrix perspective, *Phys. Rev. B* **103**, 214206 (2021).
 - [9] B. Villalonga, X. Yu, D. J. Luitz, and B. K. Clark, Exploring one-particle orbitals in large many-body localized systems, *Phys. Rev. B* **97**, 104406 (2018).
 - [10] Many-body localization of spinless fermions with attractive interactions in one dimension, *SciPost Phys.* **4**, 002 (2018).
 - [11] N. Macé, N. Laflorencie, and F. Alet, Many-body localization in a quasiperiodic Fibonacci chain, *SciPost Phys.* **6**, 050 (2019).
 - [12] M. Hopjan and F. Heidrich-Meisner, Many-body localization from a one-particle perspective in the disordered one-dimensional bose-hubbard model, *Phys. Rev. A* **101**, 063617 (2020).
 - [13] S. Pilatowsky-Cameo, I. Marvian, S. Choi, and W. W. Ho, Hilbert-space ergodicity in driven quantum systems: Obstructions and designs, *Physical Review X* **14**, 10.1103/physrevx.14.041059 (2024).
 - [14] E. J. Heller, Bound-state eigenfunctions of classically chaotic hamiltonian systems: Scars of periodic orbits, *Phys. Rev. Lett.* **53**, 1515 (1984).
 - [15] M. V. Berry, Regular and irregular semiclassical wavefunctions, *Journal of Physics A: Mathematical and General* **10**, 2083 (1977).
 - [16] F. Borgonovi, F. Izrailev, L. Santos, and V. Zelevinsky,

- Quantum chaos and thermalization in isolated systems of interacting particles, *Physics Reports* **626**, 1–58 (2016).
- [17] N. Macé, F. Alet, and N. Laflorencie, Multifractal scalings across the many-body localization transition, *Phys. Rev. Lett.* **123**, 180601 (2019).
- [18] W. Beugeling, A. Bäcker, R. Moessner, and M. Haque, Statistical properties of eigenstate amplitudes in complex quantum systems, *Phys. Rev. E* **98**, 022204 (2018).
- [19] A. De Luca and A. Scardicchio, Ergodicity breaking in a model showing many-body localization, *EPL (Europhysics Letters)* **101**, 37003 (2013).
- [20] L. F. Santos and M. Rigol, Onset of quantum chaos in one-dimensional bosonic and fermionic systems and its relation to thermalization, *Physical Review E* **81**, 10.1103/physreve.81.036206 (2010).
- [21] W. Beugeling, A. Andreanov, and M. Haque, Global characteristics of all eigenstates of local many-body hamiltonians: participation ratio and entanglement entropy, *Journal of Statistical Mechanics: Theory and Experiment* **2015**, P02002 (2015).
- [22] D. J. Luitz, N. Laflorencie, and F. Alet, Many-body localization edge in the random-field heisenberg chain, *Phys. Rev. B* **91**, 081103 (2015).
- [23] G. Misguich, V. Pasquier, and J.-M. Luck, Inverse participation ratios in the xxz spin chain, *Physical Review B* **94**, 10.1103/physrevb.94.155110 (2016).
- [24] E. Tsukerman, Inverse participation ratios in the xx spin chain, *Physical Review B* **95**, 10.1103/physrevb.95.115121 (2017).
- [25] G. De Tomasi and I. M. Khaymovich, Multifractality meets entanglement: Relation for nonergodic extended states, *Phys. Rev. Lett.* **124**, 200602 (2020).
- [26] A. Bäcker, M. Haque, and I. M. Khaymovich, Multifractal dimensions for random matrices, chaotic quantum maps, and many-body systems, *Phys. Rev. E* **100**, 032117 (2019).
- [27] D. J. Luitz, N. Laflorencie, and F. Alet, Many-body localization edge in the random-field heisenberg chain, *Physical Review B* **91**, 10.1103/physrevb.91.081103 (2015).
- [28] M. Rigol and L. F. Santos, Quantum chaos and thermalization in gapped systems, *Physical Review A* **82**, 10.1103/physreva.82.011604 (2010).
- [29] M. Haque, P. A. McClarty, and I. M. Khaymovich, Entanglement of midspectrum eigenstates of chaotic many-body systems: Reasons for deviation from random ensembles, *Phys. Rev. E* **105**, 014109 (2022).
- [30] T. I. Vanhala and T. Ojanen, Complexity of fermionic states, *Phys. Rev. Res.* **6**, 023178 (2024).
- [31] S. Boyd and L. Vandenberghe, *Convex Optimization* (Cambridge University Press, 2004).
- [32] P.-O. Löwdin, Quantum theory of many-particle systems. i. physical interpretations by means of density matrices, natural spin-orbitals, and convergence problems in the method of configurational interaction, *Phys. Rev.* **97**, 1474 (1955).
- [33] R. J. Bell, R. E. Borland, and K. Dennis, The n+2 spin-orbital approximation to the n-body antisymmetric wave function, *Journal of Physics B: Atomic and Molecular Physics* **3**, 1047 (1970).
- [34] R. E. Borland and K. Dennis, A simple approximation beyond hartree-fock, *Journal of Physics B: Atomic and Molecular Physics* **3**, 887 (1970).
- [35] D. H. Kobe, Natural orbitals, divergences, and variational principles, *The Journal of Chemical Physics* **50**, 5183 (1969), <https://pubs.aip.org/aip/jcp/article-pdf/50/12/5183/18862474/5183>.
- [36] K. Giesbertz, Are natural orbitals useful for generating an efficient expansion of the wave function?, *Chemical Physics Letters* **591**, 220–226 (2014).
- [37] J. P. Coe and M. J. Paterson, Investigating multireference character and correlation in quantum chemistry, *Journal of Chemical Theory and Computation* **11**, 4189 (2015), pMID: 26575914, <https://doi.org/10.1021/acs.jctc.5b00543>.
- [38] S. Roy and D. E. Logan, Fock-space anatomy of eigenstates across the many-body localization transition, *Phys. Rev. B* **104**, 174201 (2021).
- [39] S. Roy and D. E. Logan, Fock-space correlations and the origins of many-body localization, *Physical Review B* **101**, 10.1103/physrevb.101.134202 (2020).
- [40] P. Weinberg and M. Bukov, QuSpin: a Python package for dynamics and exact diagonalisation of quantum many body systems part I: spin chains, *SciPost Phys.* **2**, 003 (2017).
- [41] P. Weinberg and M. Bukov, QuSpin: a Python package for dynamics and exact diagonalisation of quantum many body systems. Part II: bosons, fermions and higher spins, *SciPost Phys.* **7**, 020 (2019).
- [42] CVXOPT, Python software for convex optimization, <https://cvxopt.org>, Accessed: 2025-01-21.
- [43] P. Sierant, M. Lewenstein, A. Scardicchio, L. Vidmar, and J. Zakrzewski, Many-body localization in the age of classical computing (2024), [arXiv:2403.07111 \[cond-mat.dis-nn\]](https://arxiv.org/abs/2403.07111).
- [44] F. Evers, I. Modak, and S. Bera, Internal clock of many-body delocalization, *Phys. Rev. B* **108**, 134204 (2023).
- [45] M. Altunbulak and A. Klyachko, The pauli principle revisited, *Communications in Mathematical Physics* **282**, 287–322 (2008).
- [46] R. Reuvers, Generalized pauli constraints in large systems: The pauli principle dominates, *Journal of Mathematical Physics* **62** (2021).
- [47] A. Marshall, I. Olkin, and B. Arnold, *Inequalities: Theory of Majorization and Its Applications*, Springer Series in Statistics (Springer New York, 2010).

Appendix A: Derivation of analytical upper limit results

Specializing to the case $q = 1$, we will now seek solutions to the optimization problem of Eqn. 6. Analogously to the derivation of classical statistical ensembles, we can solve the constrained maximization problem using lagrange multipliers. To this end, we write a lagrangian

$$L(\vec{p}, \vec{\mu}) = \vec{p} \cdot \log(\vec{p}) - \sum_i \mu_i \left(\sum_j p_j \lambda_{ij} - \lambda_i \right) - M \left(\sum_j p_j - 1 \right), \quad (\text{A1})$$

where the lagrange multipliers μ_i correspond to the expectation value conditions and M enforces the normalization. Taking derivatives with respect to p_i and the

lagrange multipliers we get the equations

$$\begin{aligned} \log(p_j) + 1 - \sum_i \mu_i \lambda_{ij} - M &= 0 \\ \sum_j p_j \lambda_{ij} &= \lambda_i \\ \sum_j p_j &= 1 \end{aligned} \quad , \quad (\text{A2})$$

so that

$$p_j = \exp\left(\sum_i \mu_i \lambda_{ij} + M - 1\right) = \exp\left(\sum_i \mu_i \lambda_{ij}\right) / Z, \quad (\text{A3})$$

where the normalization has been absorbed to Z . We note that the positivity conditions are automatically satisfied.

Further results require some concrete operators λ_i . A simple example is to take a fermionic many-body system with N orbitals and let $\hat{\lambda}_i$ be the occupation of the i :th orbital, $\hat{\lambda}_i = \hat{n}_i$. The basis states are Slater determinants that can be indexed by their occupation number sets $\{n_i\}$ with each $n_i = 0, 1$. Thus the weights of the maximum complexity configuration take the form

$$p_{\{n_i\}} = \exp\left(\sum_i \mu_i n_i\right) / Z, \quad (\text{A4})$$

which is of the same form as in an ensemble of free fermions with μ_i the normalized single-particle ‘‘energies’’. If we allow configurations that mix different particle numbers, the weights of the configurations are exactly those of a grand canonical ensemble of free fermions. Thus the maximal complexity is given by the well-known expression of the grand canonical entropy,

$$S_1^{max.gc} = - \sum_i (n_i \log(n_i) + (1 - n_i) \log(1 - n_i)). \quad (\text{A5})$$

This upper limit is tight in the sense that the configuration attaining the maximal complexity with the given occupations is constructed. However, this only holds in the ‘‘grand canonical’’ sense, when different particle numbers are mixed. As many-body Hamiltonians usually conserve the particle number, the bound could be made more strict by considering the canonical ensemble where only configurations with a fixed particle number are allowed. However, a simple formula for the entropy of the canonical ensemble for free fermions does not exist. In fact, when particle conservation is enforced, the constraints cannot even be satisfied if the occupation number set lies outside the polygon defined by the generalized Pauli constraints [45, 46], which indicates that the exact solution for the particle conserving case is complicated. Nevertheless, the grand canonical formula is still an upper bound for the complexity even in the particle conserving case, as it simply relaxes a constraint.

The upper bound relation $S_1 \leq S_1^{max.gc}$ immediately also gives an upper bound for the fractal dimension $D_1 = S_1 / \log(Q)$, where Q is the number of basis states in the Hilbert space. For a single-component fermion system with N_o orbitals the full space has $Q = \binom{N_o}{\nu N_o}$ states, where ν is the filling fraction, and the maximal possible complexity, obtained for the uniform distribution, is simply $\log(Q)$. From the general inequality

$$\frac{1}{n+1} \exp(nH(k/n)) \leq \binom{n}{k} \leq \exp(nH(k/n)), \quad (\text{A6})$$

where $H(p) = -p \log(p) - (1-p) \log(1-p)$, we find that

$$\begin{aligned} \log(Q) &= -N_o (\nu \log(\nu) + (1-\nu) \log(1-\nu)) \\ &\quad + O(\log(N_o)), \end{aligned} \quad (\text{A7})$$

and thus, in the limit of $N_o \rightarrow \infty$, the bound for the fractal dimension becomes

$$\lim_{N_o \rightarrow \infty} D_1^{max.gc} = \frac{\lim_{N_o \rightarrow \infty} S_1^{max.gc} / N_o}{-\nu \log(\nu) - (1-\nu) \log(1-\nu)}, \quad (\text{A8})$$

with the assumption that $S_1^{max.gc} / N_o$ converges as the system size is increased. The maximal value of $S_1^{max.gc} / N_o$ occurs with the uniform configuration where each $n_i = \nu$, and equals $-\nu \log(\nu) - (1-\nu) \log(1-\nu)$. This shows that, despite the relaxation of particle conservation, $D_1^{max.gc} \leq 1$ provides a non-trivial upper bound in the thermodynamic limit. In particular, midspectrum states of chaotic systems are expected to have $D_1 \rightarrow 1$ in the thermodynamic limit, which implies that $D_1^{max.gc}$ must approach 1.

It is also possible to obtain some analytical results for conditions involving higher correlators. For example, if we assume knowledge of some subset of the density-density correlators $\langle \psi | \hat{n}_i \hat{n}_j | \psi \rangle$, $ij \in S$, we get analogously to the above derivation

$$p_{\{n_i\}} = \exp\left(\sum_{ij \in S} \mu_{ij} n_i n_j\right) / Z, \quad (\text{A9})$$

where the summation is over the chosen subset S of pairs i, j . To find the upper bound we should then determine the lagrange multipliers μ_{ij} such that the expectation value constraints are fulfilled. The general case corresponds to solving a lattice gas problem or a classical Ising model with arbitrary coupling constants, and no analytical solution is thus available. However, we can consider e.g. the case of a 1D model in the position basis, where the well-known solution of the Ising model can be applied. If only knowledge of the average density-density correlation between nearest-neighbour orbitals is assumed, and particle conservation is again relaxed, then the result corresponds to the entropy of the 1D Ising model expressed as a function of the nearest neighbour correlation function.

Appendix B: Notes on the natural orbitals

The natural orbitals of a pure state $|\psi\rangle$ are defined as the eigenorbitals of the one-particle density matrix

$$\rho_{ij} = \langle \psi | c_i^\dagger c_j | \psi \rangle, \quad (\text{B1})$$

and the corresponding eigenvalues, i.e. the average occupations of the natural orbitals, are referred to as the natural occupations. Let us denote the occupations in some arbitrary orbital basis as n_i and the natural occupations as λ_i . We will assume that they are indexed in decreasing order such that $n_i \geq n_{i+1}$ and $\lambda_i \geq \lambda_{i+1}$. By the Schur-Horn theorem the natural occupations majorize [47] the occupations in any other orbital basis [37], meaning

$$\sum_{i=1}^k \lambda_i \geq \sum_{i=1}^k n_i, \quad (\text{B2})$$

for all $k = 1 \dots N_o$, with

$$\sum_{i=1}^k \lambda_i = \sum_{i=1}^k n_i. \quad (\text{B3})$$

We also write in vector notation $\vec{\lambda} \succ \vec{n}$. If S is any Schur-convex function, such as the Shannon entropy or any of the Renyi-entropies S_q with $q > 0$, then $S(\vec{\lambda}) \leq S(\vec{n})$ [47]. It thus follows that e.g. the occupation entropy $S_{occ} = -\sum_i n_i \log(n_i)$ is minimized in the natural orbital basis. Furthermore, if we consider the hole occupations ordered from largest to smallest, $n_i^h = 1 - n_{N_o - i + 1}$ and $\lambda_i^h = 1 - \lambda_{N_o - i + 1}$, it can be shown that the λ_i^h majorize n_i^h , or $\vec{\lambda}^h \succ \vec{n}^h$. It then follows that the hole occupation entropy $S_{occ,h} = -\sum_i (1 - n_i) \log(1 - n_i)$ and the upper bound $S_1^{max,gc} = S_{occ} + S_{occ,h}$ are also minimized in the natural orbital basis. Therefore the smallest upper bound for the complexity is obtained in the natural orbital basis.